Research in Pharmaceutical Sciences, June 2023; 18(3): 244-261
Received: 24-11-2022
Peer Reviewed: 16-01-2023
Revised: 30-01-2023
Accepted: 05-02-2023
Published: 14-03-2023

School of Pharmacy & Pharmaceutical Sciences
Isfahan University of Medical Sciences

Original Article

Formulation design and physicochemical evaluation of an anti-inflammatory hydrogel patch containing *Crinum asiaticum* L. extract

Chonthicha Kongkwamcharoen[1], Arunporn Itharat[2,3,*], Wichan Ketjinda[4], Hyang-Yeol Lee[5], Gi-Seong Moon[5], and Neal M. Davies[6]

[1]Graduate School on Applied Thai Traditional Medicine, Faculty of Medicine, Thammasat University, Pathumthani 12120, Thailand.
[2]Department of Applied Thai Traditional Medicine, Faculty of Medicine, Thammasat University, Pathumthani 12120, Thailand.
[3]Center of Excellence in Applied Thai Traditional Medicine Research (CEATMR), Thammasat University, Pathumthani 12120, Thailand.
[4]Faculty of Pharmaceutical Sciences, Prince of Songkla University, Thailand.
[5]Department of Biotechnology, Korea National University of Transportation, 61 Daehak-ro, Jeungpyeong-gun, Chungbuk, 27909, Republic of Korea.
[6]Faculty of Pharmacy and Pharmaceutical Sciences, University of Alberta, Edmonton, Canada.

Abstract

Background and purpose: *Crinum asiaticum* L. has long been used in Thai traditional medicine to treat osteoarthritis and inflammation by placing it on painful areas without further formulation design which is suboptimal for therapeutic use. Thus, this research aims to formulate a topical hydrogel patch containing *C. asiaticum* L. extracts (CAE) for anti-inflammatory effects.
Experimental approach: The hydrogel patches are made from carrageenan, locust bean gum, with glycerin as a plasticizer and contain CAE formulated by using response surface methodology based on Box-Behnken design for design, determination of the effect of independent factors on the tensile strength, and optimization of the hydrogel patch formulation. *In vitro* release and skin permeation studies using a modified Franz diffusion cell and anti-inflammatory activity were evaluated.
Findings/Results: The optimized CAE hydrogel patch showed a good correlation between predicted and observed tensile strength values and exerted its maximum cumulative lycorine release and permeation at 69.38 ± 2.78% and 48.51 ± 0.45%, respectively which were fit to Higuchi's kinetic model. The release rates were found to decrease with an increase in the polymer proportion of carrageenan and locust bean gum. In addition, the patch exerted potent *in vitro* anti-inflammatory activity with an IC_{50} value of 21.36 ± 0.78 µg/mL.
Conclusion and implication: The optimized CAE hydrogel patch application was successfully formulated with excellent mechanical properties, cumulative release, permeation, and anti-inflammatory effects. Thus, it has the potential to be further developed as a herbal application to relieve pain and inflammation. The *in vivo* anti-inflammatory effect of this delivery system should be further investigated.

Keywords: Anti-inflammatory; *Crinum asiaticum* L.; Evaluation; Formulation design; Hydrogel patch; Optimization.

INTRODUCTION

Osteoarthritis (OA) is the most common chronic degenerative disease in elderly people around the world involving synovial fluid modification, tissue inflammation, and cartilage erosion (1). Inflammation is a physiologic response to protect cells from pathogens and injury. However, prolongation of the inflammatory responses leads to damage of cells, tissues, and organs and leads to chronic inflammatory diseases (2).

*Corresponding author: A. Itharat
Tel & Fax: +66-29269749
Email: iarunporn@yahoo.com

Access this article online

Website: http://rps.mui.ac.ir

DOI: 10.4103/1735-5362.371581

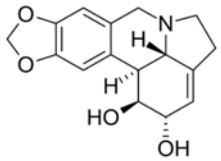

Fig. 1. The molecular structure of lycorine.

The inflammatory mediators such as nitric oxide, prostaglandin E_2, and tumor necrosis factor-alpha destroy cartilage, which manifests clinically as symptoms of OA including pain, swelling, and stiffness (3,4). Corticosteroids and nonsteroidal anti-inflammatory drugs (NSAIDs) are prevalent treatments for OA. However, taking corticosteroids and NSAIDs for a long time may have adverse effects, particularly in the heart, kidneys, and gastrointestinal tract (5-7).

Crinum asiaticum L. (Amaryllidaceae family) has long been used in Thailand and Asia to relieve pain in inflamed joints as an inflammatory disease treatment (8,9). Previous research has delineated the bioactivity of *C. asiaticum* L. which includes antioxidant and anti-inflammatory activity (10-12) and also showed a significant anti-inflammatory effect *in vivo* as measured by inhibition of paw edema 51.60 ± 2.50% at the first hour and 40.80 ± 0.52% at the fourth hour after administration (13). Lycorine (Fig. 1) is the most common *Crinum* alkaloid that has potent anti-tumor, immunological, and anti-inflammatory activities (14-16). *In vivo*, lycorine has also been shown to decrease autophagy in osteoclasts (17).

In Thai folk medicine, *C. asiaticum* L. is used as a topical treatment for muscular pain, injuries, and inflamed joints. The guidelines for certification of folk medicine reveal that fresh leaves of *C. asiaticum* L. are grilled on a charcoal stove and are then applied to cover areas that are sources of pain (18). However, the use of traditional folk medicine may not be a comfortable treatment method for some patients. Our study was designed to develop a more convenient topical form.

Topical drug delivery systems applied *via* the skin, have the advantage of a lack of first-pass metabolism and the drug can be preferentially delivered to the site of action (19). Thai traditional medicine already includes many topical dosage forms to treat osteoarthritis including herbal medicine placed on the knee, herbal ball compress, oils, gels, and creams. However, those dosage forms have disadvantages in their use, decreased efficacy when adhering to clothing and uncontrolled drug release. Therefore, a controlled-release patch formulation that has a low frequency of application can prolong the duration of action and is more convenient to use and portable with reduced loss of adhering drug has several distinct advantages (20). Furthermore, hydrogels are three-dimensional (3D) networks of polymers that contain high amounts of water, which are preferential for inflamed skin areas due to their ability to moisturize the skin, provide a cooling effect, and reduce the redness and heat evident in inflamed areas (21). For these reasons, a hydrogel patch containing *C. asiaticum* L. extract (CAE) was developed for use as an anti-inflammation application.

In the design of drug formulations, the contemporary approach employed to optimize formulation would be to avoid all unpredictable factors that may affect the cost of production. Hence, the design of experiments with response surface methodology (RSM) is used as a modern systematic approach in pharmaceutical development techniques designed to determine the relationships between independent variable factors affecting one or more dependent variables through the use of mathematical models (22,23). RSM and design of experiments statistical software are effective tools that help to reduce the experimental runs, save time, and can predict and optimize the process and the product (24,25). Recently, RSM has been used to optimize formulation design in pharmaceutical development (26).

Therefore, this research aims to develop hydrogel patches made from carrageenan, locust bean gum with glycerin as a plasticizer, and containing CAE by using RSM for formulation and optimization of hydrogel patch formulation. *In vitro* release and skin permeation studies were undertaken using a Franz diffusion cell. The hydrogel patches were evaluated using scanning electron microscopy (SEM), Fourier-transform infrared spectroscopy (FTIR), differential scanning calorimetry (DSC), and X-ray diffraction (XRD). Moreover, the anti-inflammatory activity through inhibition of nitric oxide

production in RAW 264.7 cells was used to confirm the anti-inflammatory effects of the hydrogel patch.

MATERIALS AND METHODS

Materials and chemicals

C. asiaticum L. leaves, specimen voucher (SKP-008 03 01 01) was collected from the Faculty of Medicine, Thammasat University, Pathumthani, Thailand. The specimen voucher was deposited at the herbarium of the Southern Center of Thai Medicinal Plants, Faculty of Pharmaceutical Sciences, Prince of Songkla University, Thailand. Carrageenan and Locust bean gum were purchased from Beauty Cosmetic Co., Ltd., Korea. Glycerin was purchased from Sigma-Aldrich, USA. Standard lycorine (purity > 98%) was purchased from Chem Faces (Wuhan, China). Triethylamine, phosphoric acid, dimethyl sulfoxide (DMSO), and purified water were prepared by Milli Q® system from Millipore (Bedford, MA, USA). Acetonitrile high-performance liquid chromatography (HPLC) grade was purchased from RCI LabScan (Bangkok, Thailand). 3-(4, 5-dimethyl-2-thiazolyl)-2,5-diphenyl-2H-tetrazolium bromide (MTT) was purchased from Sigma (MO, USA). The murine macrophage leukemia cell line (RAW 264.7: ATCC® TIB-71™) was purchased from American Type Culture Collection (ATCC®, VA, USA).

Preparation of extract

The dried leaves were macerated with 95% ethanol for three days and then filtered through a Whatman No.1 filter paper. The crude extract was dried by a rotary evaporator and the residue was macerated two additional times.

Experimental design

RSM based on the Box-Behnken design (BBD; Design-Expert software, Stat-Ease Inc., Minneapolis, MN, USA) was used for optimizing the formulation (24,27). The BBD consists of three-level-three-factor (X_1 = carrageenan, X_2 = locust bean gum, and X_3 = glycerin) were used to evaluate the effects of independent variables on a response of the tensile strength of the hydrogel patches. Variables with their levels of BBD are presented in Table 1 and the composition from the randomized run in BBD is shown in Table 2.

Table 1 Code and actual of independent variables/levels of Box-Behnken design.

Independent variables	Code of independent variables/levels			Actual independent variables/levels		
Carrageenan (X_1)	-1	0	1	0.5	1.25	2
Locust bean gum (X_2)	-1	0	1	0.5	1.25	2
Glycerin (X_3)	-1	0	1	0.2	0.5	0.8

Table 2. The composition from the randomized run in Box-Behnken design is shown in code and the actual independent variable levels.

Formulation	Code of independent variables/levels			Actual independent variables/levels		
	X_1	X_2	X_3	X_1	X_2	X_3
F1	-1	0	-1	0.50	1.25	0.20
F2	0	-1	+1	1.25	0.50	0.80
F3	0	-1	-1	1.25	0.50	0.20
F4	0	0	0	1.25	1.25	0.50
F5	+1	0	+1	2.00	1.25	0.80
F6	0	+1	+1	1.25	2.00	0.80
F7	0	0	0	1.25	1.25	0.50
F8	0	0	0	1.25	1.25	0.50
F9	-1	0	+1	0.50	1.25	0.80
F10	+1	-1	0	2.00	0.50	0.50
F11	-1	+1	0	0.50	2.00	0.50
F12	-1	-1	0	0.50	0.50	0.50
F13	0	0	0	1.25	1.25	0.50
F14	0	0	0	1.25	1.25	0.50
F15	0	+1	-1	1.25	2.00	0.20
F16	+1	+1	0	2.00	2.00	0.50
F17	+1	0	-1	2.00	1.25	0.20

X_1, Carrageenan; X_2, locust bean gum; X_3, glycerin.

Preparation of herbal medicine hydrogel patch

Hydrogel patches were prepared by following variable proportions from BBD (Table 2) (Thai Petty Patent Application Number 2203000378). Carrageenan (X_1) and locust bean gum (X_2) were solubilized in distilled water by a homogenizer until all particles dissolved completely and homogeneously. Subsequently, glycerin (X_3) as a plasticizer was added. CAEs (2%, w/w) were added slowly and stirred until uniformity. A solution of KCl (0.1%, w/w) and Uniphen™ were added for crosslinking and as a preservative. The matrix solution obtained was transferred to an ultrasonicator for degasifying and then poured onto a glass with a micrometer film applicator to drag it and form the hydrogel patch. The CAE hydrogel patches were kept in an aluminum foil bag in a refrigerator at 4 °C.

Determination of physicochemical properties of hydrogel patch

Thickness

The thickness of the hydrogel patches was measured using a Teclock® dial thickness gauge micrometer at three different places on a single hydrogel patch of each formulation (n = 3).

Tensile strength and elongation at break

The mechanical properties such as tensile strength (kg/cm^2), and percent of elongation at break were evaluated using a texture analyzer (TA. XT plus, Stable Micro Systems, USA) with a 5 kg load cell. Following the method modified from the early study (28), the hydrogel patch specimen of specific dimension (1 × 4 cm^2) was fixed between two clamps and positioned and tested as follows: pre-test speed of 1 mm/s, test speed of 1 mm/s, trigger force 5 g. The results of tensile strength and elongation at break were calculated by using the Exponent lite program and the data were measured in triplicate of each hydrogel patch.

Scanning electron microscopy

The scanning electron microscope (SEM; JSM-5410LV, JEOL, Japan) with a high voltage of 20 kV was used to study the surface and cross-section morphology of the hydrogel patch. The surface and cross-section of the blank hydrogel patch and the optimized CAE hydrogel patch were incubated at 45 °C for 48 h, then placed on a copper stub and coated with gold in a sputter coater before testing.

FTIR spectroscopy

FTIR Spectrometer (Nicolet iS50, Thermo Scientific, USA) was used to analyze FTIR spectroscopy of CAE, standard lycorine, carrageenan, locust bean gum, blank hydrogel patch, and the optimized CAE hydrogel patch. The blank hydrogel patch and the optimized CAE hydrogel patch were incubated at 45 °C for 48 h before testing by using 64 scans at a resolution of 4 cm^{-1} from wave number region of 4,000 to 400 cm^{-1}.

DSC

The DSC study was used to investigate the compatibility of components in the hydrogel patch. The blank hydrogel patch and the optimized CAE hydrogel patch were incubated at 45 °C for 48 h before testing. The DSC thermograms of carrageenan powder, locust bean gum powder, blank hydrogel patch, and the optimized CAE hydrogel patch were carried out on a DSC instrument (DSC 3+, Mettler Toledo, Switzerland) under a liquid nitrogen atmosphere and scanned at the heat flow from 20 °C to 350 °C with a heating rate of 10 °C /min.

XRD

The XRD study was used to characterize the crystallinity of carrageenan powder, locust bean gum powder, blank hydrogel patch, and the optimized CAE hydrogel patch by using XRD (model: AERIS, Malvern Panalytical, Netherlands). The blank hydrogel patch and optimized CAE hydrogel patch were incubated at 45 °C for 48 h before the test. The current for the X-ray source and generator operating voltage was set at 15 mA and 40 kV, respectively, with an angle range of 5-40° (2θ) and a stepped angle of 0.02° (2θ)/s (29).

Drug content of CAE hydrogel patch

The optimized CAE hydrogel patch was dissolved in solvent then sonicated for 45 min and centrifuged at 5,000 rpm for 20 min. The solution was filtered through a membrane filter before analysis of the lycorine content by HPLC.

In vitro release and permeation study

The *in vitro* release and skin permeation of lycorine from CAE hydrogel patches were determined in triplicate by using a modified Franz diffusion cell method from a previous study (30). The cellulose dialysis membrane (molecular weight cut-off 12,000 to 14,000 Da, Cellu Sep T4, Membrane Filtration Product, Inc., USA) was soaked for 30 min in a medium and then placed between the donor and receptor compartments. The buffer solution containing ethanol (20% v/v) in phosphate-buffered saline solution pH 7.4, was maintained at 37 ± 1 °C and continuously stirred by a magnetic stirrer. The CAE hydrogel patches were cut to cover the diffusion area and placed on the cellulose dialysis membrane. The receptor medium was withdrawn at set time intervals and immediately replaced with an equal volume of fresh medium. The lycorine content was analyzed using HPLC. For the permeation study, the method was performed in a similar manner as the drug release but replaced the cellulose dialysis membrane with pig ear skin that was prepared by the Prince of Songkla University, Thailand (31).

HPLC analytical

The HPLC system (Agilent® 1200; Agilent Technologies, USA) and C18 reverse phase column (Zorbax® C18, 4.6 × 250 mm, 5 µ) were used to analyze lycorine content according to the method of Kongkwamcharoen and co-workers (11) and detected by diode array detector at the wavelength of 290 nm.

Anti-inflammatory activity by inhibition of nitric oxide production from RAW 264.7 cells and cytotoxicity by MTT assay

This study was determined according to the modified method of Makchuchit and co-workers (32). RAW264.7 cells were cultured in Dulbecco's modified eagle medium and incubated at 37°C with 5% CO_2. The cells were seeded into 96-well plates and incubated for 24 h. Lipopolysaccharide at the final concentration of 5 ng/mL was used to treat the cells. Each sample, prepared at various concentrations (0.1-100 µg/mL), was then added and incubated for 24 h. Subsequently, the Griess reagent was added. The plate optical density was measured at 570 nm by a microplate reader. MTT solution was used to treat cells to determine their viability. The inhibition % and toxicity % were calculated. The half inhibitory concentration (IC_{50}) was calculated by using GraphPad Prism software (CA, USA).

Statistical analysis

All data are the mean of three replications. Values of different parameters are expressed as the mean ± SEM or mean value ± SD.

RESULTS

Evaluations of mechanical properties

The mechanical properties of 17 formulations of CAE hydrogel patches are shown in Table 3.

Table 3. Results of mechanical properties of *Crinum asiaticum* L. extract hydrogel patch. Data are expressed as mean ± SD

Formulation	Thickness (mm)	Tensile strength (kg/cm^2)	Elongation at break (%)
F1	0.45 ± 0.01	0.61 ± 0.18	185.77 ± 21.71
F2	0.49 ± 0.02	0.56 ± 0.35	137.36 ± 22.36
F3	0.51 ± 0.01	1.38 ± 0.78	181.77 ± 40.34
F4	0.57 ± 0.01	1.79 ± 0.07	250.01 ± 07.02
F5	0.58 ± 0.01	2.06 ± 0.33	220.06 ± 25.18
F6	0.59 ± 0.01	2.31 ± 0.46	226.52 ± 06.81
F7	0.56 ± 0.01	1.78 ± 0.32	246.09 ± 42.03
F8	0.57 ± 0.01	1.79 ± 0.03	271.47 ± 09.49
F9	0.44 ± 0.01	0.73 ± 0.13	200.38 ± 38.04
F10	0.49 ± 0.02	1.15 ± 0.23	146.44 ± 09.88
F11	0.45 ± 0.01	0.97 ± 0.19	239.19 ± 30.20
F12	0.42 ± 0.02	0.39 ± 0.23	132.14 ± 08.05
F13	0.57 ± 0.02	1.80 ± 0.19	257.34 ± 20.42
F14	0.56 ± 0.01	1.99 ± 0.14	253.64 ± 08.05
F15	0.58 ± 0.02	1.86 ± 0.75	205.73 ± 41.01
F16	0.59 ± 0.01	2.33 ± 0.12	242.43 ± 10.22
F17	0.59 ± 0.01	1.69 ± 0.09	203.87 ± 09.92

The thickness of all hydrogel patches varied between 0.42 ± 0.02 to 0.59 ± 0.01 mm. Tensile strength values were found to be in the range of 0.39 ± 0.23 kg/cm^2 to 2.33 ± 0.12 kg/cm^2 and the range of 132.14 ± 8.05 to 271.47 ± 9.49 were exerted in % elongation at break values, as a result of the formulation factors, *i.e.* polymer proportion and amount of plasticizer which will be discussed further.

Statistical analysis of the model and effect of formulation variables on tensile strength of CAE hydrogel patches

The formulation of the CAE hydrogel patch was optimized by using RSM to study the interactions and its effects between selected variables (24,27). A total of 17 formulations with independent variables were evaluated for tensile strength as shown in Table 3 and were used to analyze the variance by using the Design-expert software (Stat-Ease Inc., Minneapolis, MN, USA). Experimental data were fitted to different polynomial models and were tested statistically by lack of fit and model summary statistics to determine the robustness of the models (Table 4). There was a lack of fit in linear regression and the 2FI model, not in the quadratic model. Moreover, the quadratic model was observed to be the best fit for the tensile strength responses with the coefficient of determination (R^2) = 0.9742 (Table 4). The adequacy of the model was also confirmed with an analysis of variance (ANOVA). The experimental data were analyzed by ANOVA and the significance was assessed by the corresponding *P*-value of the regression coefficients (Table 5). The quadratic model demonstrated a $P < 0.0001$ and the quadratic model was found to be the best fit for the response tensile strength. In this case, A, B, BC, A^2, and B^2 were significant model terms (Table 5). The final equation in terms of actual factors was generated by design expert software as the following quadratic equation (1)

$$\text{Tensile strength (kg/cm}^2) = -0.55 + 2.23A + 0.44B - 0.73C + 0.27AB + 0.28AC + 1.41BC - 0.78A^2 - 0.32B^2 - 1.33C^2 \quad (1)$$

The magnitude and direction of factor coefficients in equation (1) describe the effect of factors (A, B, C) on the response. The factor having the greater magnitude shows a strong effect on the response. The equation describes that factors A (carrageenan) and B (locust bean gum) have positive effects on the tensile strength of hydrogel patches. Factor A has an influence on the hydrogel patch's tensile strength compared to factor B with a coefficient value of 2.23. In contrast, the response decreased when factor C (glycerin) had an increase in negative coefficients. In addition, the interaction factors AB, AC, and BC have synergistic effects on increasing tensile strength. However, a two-fold change in each of factors A, B, and C revealed negative effects on the tensile strength and indicated that an excess of those factors affects a decrease in the tensile strength of hydrogel patches.

Table 5. ANOVA for response surface quadratic model.

Source	Sum of squares	*P*-value
Model	6.15	< 0.0001
A	2.57	< 0.0001
B	1.99	< 0.0001
C	0.0018	0.7889
AB	0.09	0.0898
AC	0.02	0.4394
BC	0.40	0.0042
A^2	0.81	0.0006
B^2	0.14	0.0437
C^2	0.06	0.1504

A, Carrageenan; B, locust bean gum; C, glycerin

Table 4. Summary of lack of fit and model statistics.

Source	Sum of squares	*P*-value, Probability > F	Standard deviation	R^2	Adjusted R^2
Lack of fit					
Linear	1.72	0.0040	-	-	-
2FI	1.22	0.0039	-	-	-
Quadratic	0.13	0.0683	-	-	-
Cubic	0.000	-	-	-	-
Pure Error	0.032	-	-	-	-
Model statistics					
Linear	-	-	0.37	0.7217	0.6575
2FI	-	-	0.35	0.8023	0.6837
Quadratic	-	-	0.15	0.9742	0.9411

The 3D response surface plots on the tensile strength of CAE hydrogel patches

The 3D response surface plots were generated by the Design-expert software (Fig. 2). The effect of carrageenan (A) and locust bean gum (B) at the mid-point of the amount of plasticizer (C) on the response tensile strength is exhibited in Fig. 2A. The results determined that both factors A and B affected the tensile strength. An increasing amount of carrageenan and locust bean gum affected the tendency to increase the tensile strength, however, an excess of factors A or B in the hydrogel patch composition resulted in lower tensile strength than the hydrogel patch combined with a high proportion of both in the composition.

The effect of carrageenan (A) and glycerin (C) at the mid-point of locust bean gum (B) on the response was shown in Fig. 2B. The 3D surface plots illustrate that carrageenan influenced tensile strength to a greater extent than glycerin. The effect of carrageenan at any amount of glycerin was more pronounced and a trend to increase tensile strength was evident compared to the effect of glycerin at any carrageenan level. However, excess carrageenan had a tendency to decrease the tensile strength.

The effect of the interaction between locust bean gum (B) and glycerin (C) at the mid-point of factor A on the response is shown in Fig. 2C. The results indicate that locust bean gum affected the tensile strength trend to increase similar to carrageenan. However, the effect of interaction by increasing glycerin affected the increase of tensile strength which was more pronounced at the high level for the locust bean gum than carrageenan. In the case of locust bean gum, increasing amounts of glycerin at high levels of locust bean gum increased tensile strength but adversely affected tensile strength to slightly decrease at the low level of this gum. The results showed that glycerin as the plasticizer affects a decrease in tensile strength and increases flexibility in the hydrogel patch.

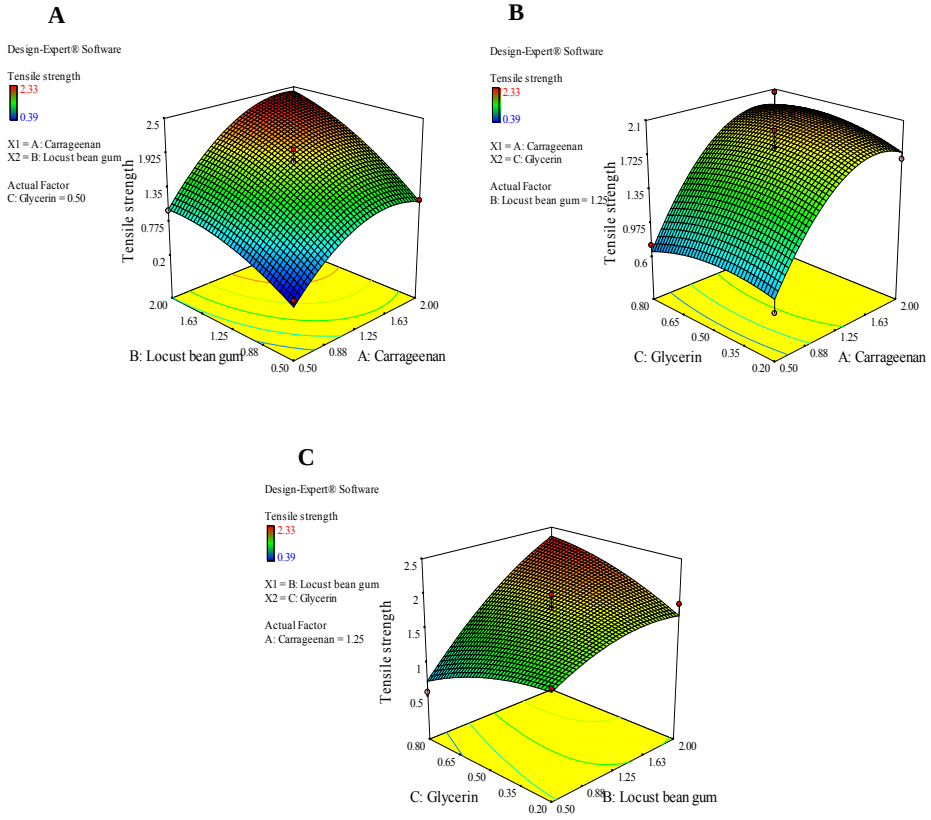

Fig. 2. The 3D response surface plots showing the effects of interaction between factors on the tensile strength including (A) carrageenan: locust bean gum, (B) carrageenan: glycerin, and (C) locust bean gum: glycerin.

Optimization of CAE hydrogel patch formulation

RSM was used for the optimization of CAE hydrogel patch formulation. Table 3 shows the mechanical properties of the CAE hydrogel patch such as tensile strength and elongation at break, which are desirable for mechanical resistance and measure of the ductility of the hydrogel patch, respectively. The tensile strength was selected as the key parameter to be optimized. The optimization was designed to set a goal as a tensile strength value of more than 1.7 kg/cm^2 and a desirability close to 1. The optimization formulation was found to be carrageenan: locust bean gum (1:1) and 0.80 of glycerin, which predicted that the value of the tensile strength would be 1.725 kg/cm^2 with a desirability value of 1. Optimization of the formulation was performed for validation purposes. The tensile strength and elongation at the break of the optimized formulation obtained values of 1.67 ± 0.12 kg/cm^2 and 270.89 ± 16.97 %, respectively. A good correlation of resultant tensile strength was displayed between the observed and predicted optimized formulation with a *P*-value of 0.57. Analyses using Student's t-test indicated that the tensile strength value was not significantly different between groups indicating that the optimized CAE hydrogel patch had the required mechanical property. F5 and F6 CAE hydrogel patches exerted tensile strength values greater than 1.7 kg/cm^2 with a high drug content. Thus, the optimized CAE hydrogel patch had carrageenan: locust bean gum (1:1) and 0.80 of glycerin, F5 and F6 formulations were selected for further study.

Drug content

The lycorine content of F5, F6, and the optimized CAE hydrogel patches were analyzed with the HPLC method. They exerted 90.38 ± 0.10, 91.21 ± 5.02, and 93.36 ± 0.72 %, respectively.

In vitro drug release study

The lycorine release of three different formulations, *i.e.* F5 (high carrageenan proportion), F6 (high locust bean gum proportion), and the optimized CAE hydrogel patch are shown in Fig. 3. The optimized CAE hydrogel patch exerted the maximum cumulative lycorine release after 6 h for 69.38 ± 2.78%. F6 and F5 hydrogel patches were obtained at the 6 h with 59.07 ± 4.13%, and 54.48 ± 2.58%, respectively.

The release kinetics model of the optimized CAE hydrogel patch exerted a more optimal fit to Higuchi's model than the zero-order and first-order models with $R^2 = 0.9684$ (Table 6). The release behavior might be a consequence of the matrix patch which absorbs the moisture then undergoes erosion, the porosity and creation of space, and a large free volume of the lycorine in the matrix patch may provide more rapid diffusion. From the results, the optimized CAE hydrogel patch showed the highest lycorine content and cumulative lycorine release. Hence, the optimized CAE hydrogel patch was selected for further study of *in vitro* skin permeation, physicochemical properties, and anti-inflammatory activity.

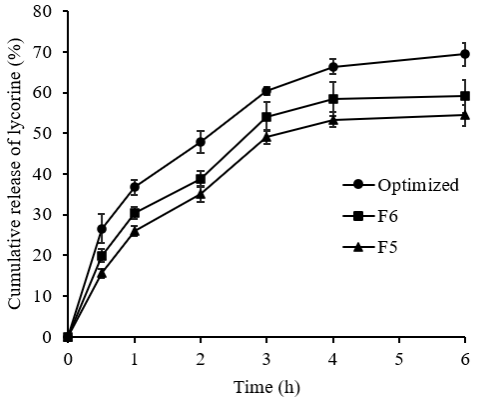

Fig. 3. The *in vitro* drug release of F5, F6, and optimized CAE hydrogel patch by using a modified Franz diffusion cell. CAE, *Crinum asiaticum* L. extract.

Table 6. Coefficient of determination from linear regression analyses of various kinetic models for *in vitro* release and skin permeation of *Crinum asiaticum* L. extract hydrogel patches.

In vitro	Hydrogel patches	Zero order $Q_t = K_0t + Q_0$	First order ($Q_t = Q_0e^{-Kt}$)	Higuchi ($Q_t = K_H\sqrt{t}$)
Release	F5	0.8221	0.8736	0.9632
	F6	0.7993	0.8625	0.9594
	Optimized	0.7940	0.8994	0.9684
Permeation	Optimized	0.7566	0.8239	0.8950

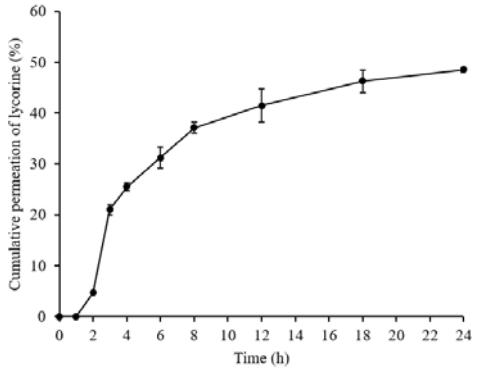

Fig. 4. The *in vitro* skin permeation of lycorine from the optimized CAE hydrogel patch by using a modified Franz diffusion cell with 20% v/v ethanol in phosphate-buffered saline. CAE, *Crinum asiaticum* L. extract.

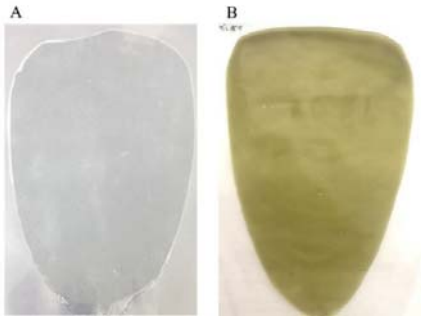

Fig. 5. (A) Blank hydrogel patch (without *Crinum asiaticum* L. extract) and (B) the optimized CAE hydrogel patch. CAE, *Crinum asiaticum* L. extract.

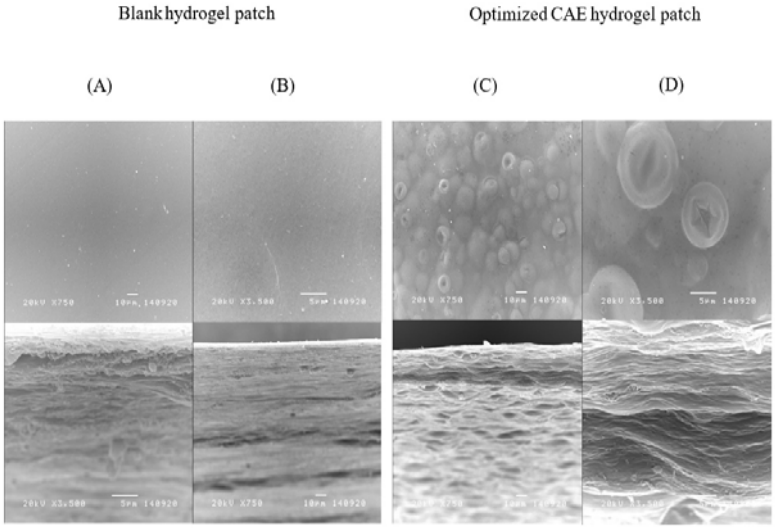

Fig. 6. Surface (upper) and cross-section (lower) (A) X750 and (B) X3,500 morphology of a blank hydrogel patch and surface (upper) and cross-section (lower) (C) X750 and (D) X3,500 morphology of the optimized CAE hydrogel patch. CAE, *Crinum asiaticum* L. extract.

In vitro skin permeation study

The *in vitro* skin permeation study was carried out by a modified Franz diffusion cell using pig ear skin as a partition membrane. From Fig. 4, the optimized CAE hydrogel patch showed an initial lycorine permeation at 2 h. However, it demonstrated the maximum cumulative lycorine permeation of 48.51 ± 0.45% at 24 h. The skin permeation kinetics model of the optimized CAE hydrogel patch provided a better fit to Higuchi's model with $R^2 = 0.8950$ (Table 6).

Evaluations of physicochemical properties of the hydrogel patch

Physical appearance

The blank hydrogel patch was transparent and colorless, while the optimized CAE hydrogel patch was a visible green color and the surface of the hydrogel patch was smooth to the touch (Fig. 5).

SEM

The surface and cross-section morphology of the blank hydrogel patch and optimized CAE hydrogel patch carried out by the SEM technique are shown in Fig. 6. The surface of the blank hydrogel patch appeared homogeneously smooth without porosity (Fig. 6A and B, upper). The cross-section of the blank hydrogel patch showed a dense layer and smooth film (Fig. 6A and B, lower). The surface of the optimized CAE hydrogel patch showed several vesicles, with the CAE inside the hydrogel matrix (Fig. 6 C and D, upper). The cross-section of the optimized CAE

hydrogel patch showed a rough, dense, and compact film (Fig. 6C and D, lower). These results support that CAE was completely loaded and dispersed in the hydrogel patch matrix.

FTIR spectroscopy

FTIR spectra of lycorine, CAE, the optimized CAE hydrogel patch, blank hydrogel patch, carrageenan, and locust bean gum are shown in Fig. 7. The spectrum of the blank hydrogel patch revealed the characteristic bands as well as the vibration of O-H at 3381.71 cm^{-1}, C-H stretching at 2900-3000 cm^{-1}, and ester sulfate groups at 1223.3 cm^{-1} in the spectrum of carrageenan, and vibration of O-H at 3330.30 cm^{-1} and aliphatic C-H at 2913.44 cm^{-1} in the spectrum of locust bean gum. Chemical interaction between carrageenan and locust bean gum can be observed by the shift in peaks corresponding to the C-O stretching band of the C-O-H group band from 1155 cm^{-1} (carrageenan) to 1151 cm^{-1} (blank hydrogel patch). The spectrum of lycorine, as a standard marker, with evident absorption peaks of stretching vibrations at 3322.31, 2927.46, and 820-700 cm^{-1} related to -OH groups, aliphatic C-H, and aromatic ring, respectively.

FTIR spectra analysis revealed thatlycorine, CAE, and the optimized CAE hydrogel patches demonstrated similar characteristic band positions at 3310-3322, 2924-2927, and 820-700 cm^{-1}. The results indicate that lycorine, an active marker of the CAE was dispersed in the hydrogel patch matrix.

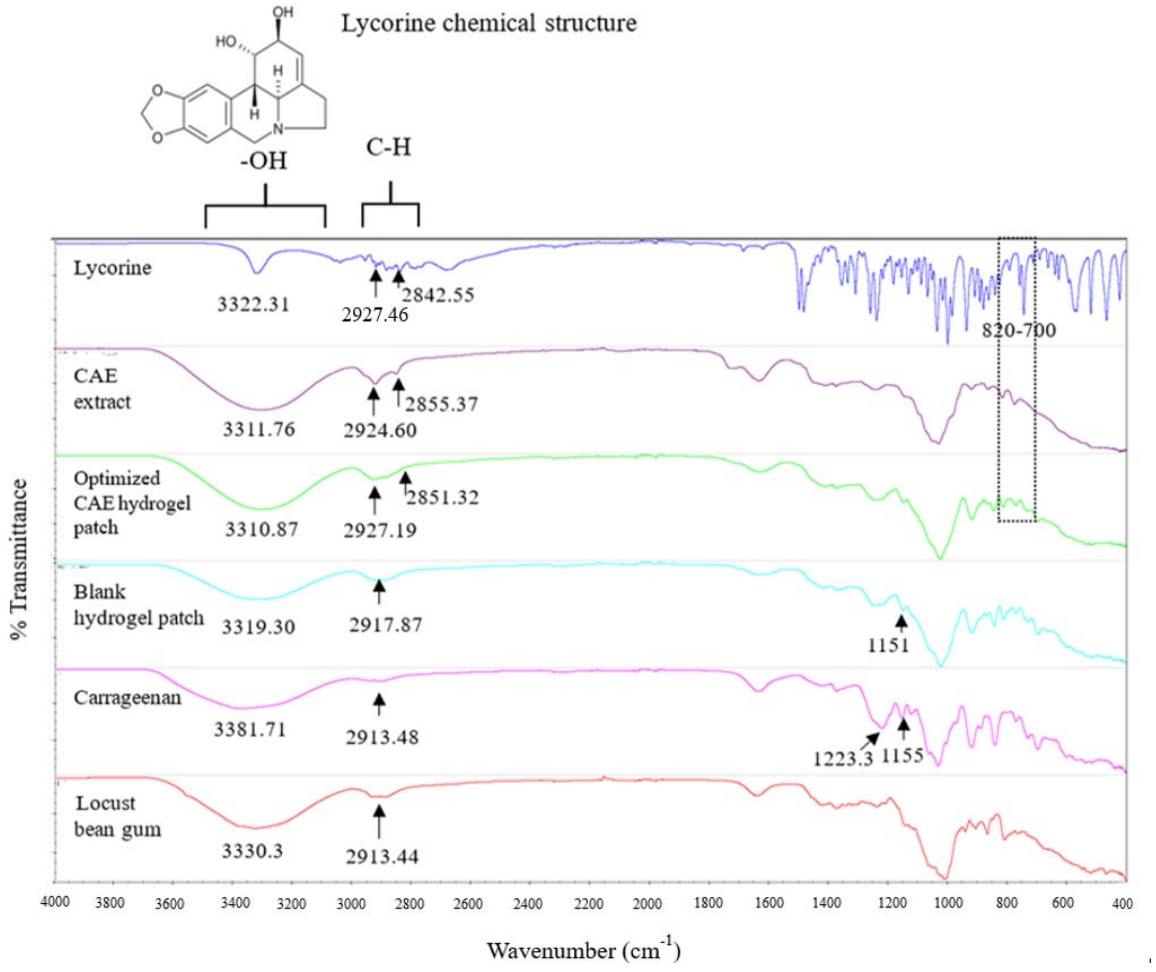

Fig. 7. The spectrum of lycorine, CAE extract, the optimized CAE hydrogel patch, blank hydrogel patch, carrageenan, and locust bean gum. CAE, *Crinum asiaticum* L. extract.

DSC

The DSC thermogram of carrageenan powder, locust bean gum powder, blank hydrogel patch, and the optimized CAE hydrogel patch were shown in Fig. 8. The DSC thermogram of locust bean gum powder was observed at 78.81 °C and melting point at 190.41 °C. Endothermic peaks for carrageenan powder showed an endothermic peak at 97.59 °C and a melting point at 147.14 °C. Carrageenan powder showed an exothermic peak at 199.57°C, which represents their degradation. The analysis thermogram of the blank hydrogel patch revealed an endothermic peak at 93.78 °C, which is between those of the pure carrageenan and locust bean gum. The melting point was observed at 206.61 °C. The optimized CAE hydrogel patch revealed high broad endothermic peaks at 94.59 °C and 189.40°C (melting point). The result showed that the DSC thermograms of the blank and optimized CAE hydrogel patch had no disguised signal. Thus, all the constituents in the blank and optimized CAE hydrogel patch were compatible.

XRD

The XRD pattern of carrageenan powder showed many sharp peaks and high intensity such as 9°, 21°, and 27° (2θ) (Fig. 9). The XRD profile of locust bean gum powder revealed sharp peaks with a broad region such as 7°, 18°, 19° and 24° (2θ) representing crystalline and amorphous characteristics. The XRD patterns of the blank hydrogel patch and the optimized CAE hydrogel patch demonstrated a broad diffraction region at 20° (2θ) and no sharp peaks representing their amorphous characters.

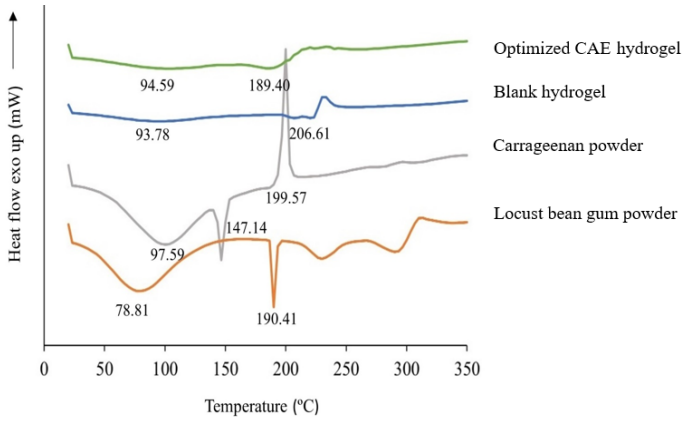

Fig. 8. The differential scanning calorimetry thermogram of the optimized CAE hydrogel patch, blank hydrogel patch, carrageenan powder, and locust bean gum powder. CAE, *Crinum asiaticum* L. extract.

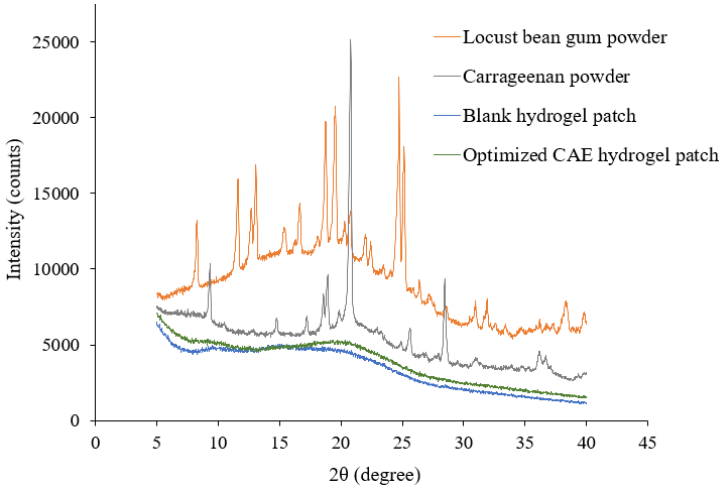

Fig. 9. X-ray diffraction patterns of locust bean gum powder, carrageenan powder, blank hydrogel patch, and optimized CAE hydrogel patch. CAE, *Crinum asiaticum* L. extract.

Table 7. Inhibitory effect on lipopolysaccharide-induced nitric oxide production from RAW 264.7 cells (% inhibition and toxicity to cells at various concentrations (μg/mL)). Data are expressed as mean ± SEM, n = 3.

Sample	[% Inhibition of nitric oxide] and (% toxic to cells)									IC_{50} (μg/mL)
	0.1	0.2	0.4	0.8	1	10	30	50	100	
Blank hydrogel patch	-	-	-	-	[-10.45 ± 0.79] (-6.95 ± 1.43)	[-5.73 ± 2.79] (6.77 ± 2.65)	[-4.89 ± 0.79] (6.70 ± 3.07)	[-3.36 ± 0.69] (16.76 ± 3.54)	-	NA
Optimized CAE hydrogel patch	-	-	-	-	[-9.42 ± 2.51] (-9.02 ± 0.84)	[11.63 ± 1.32] (-1.66 ± 4.97)	76.85 ± 3.88 (2.81 ± 3.00)	[94.51 ± 2.46] (15.24 ± 2.78)	-	21.36 ± 0.78
Prednisolone	[30.02 ± 5.70] (2.65 ± 3.05)	-	-	-	[46.52 ± 1.30] (6.21 ± 3.28)	[61.60 ± 7.46] (8.12 ± 4.95)	-	[77.86 ± 3.54] (12.54 ± 1.85)	-	1.22 ± 0.07
Diclofenac	-	-	-	-	-	-	-	[-10.01 ± 0.58] (-17.23 ± 3.34)	[1.65 ± 0.73] (-10.19 ± 1.67)	> 100
Lycorine	[-8.06 ± 2.60] (4.73 ± 2.33)	[8.32 ± 0.78] (15.95 ± 2.23)	[49.11 ± 1.28] (17.64 ± 2.58)	[79.20 ± 0.48] (25.46 ± 0.60)	[86.24 ± 3.04] (38.70 ± 2.45)	-	-	-	-	0.41 ± 0.01

– Means not tested; NA, not active.

In addition, the broad diffraction region at 20° (2θ) of the blank hydrogel patch became broader when compared with the XRD patterns of carrageenan and locust bean gum powder indicating that a change in the crystal property due to the formation of hydrogel from both gums.

Anti-inflammatory activity by inhibition of nitric oxide production and cytotoxicity on RAW 264.7 cells

As shown in Table 7, the blank hydrogel patch was inactive in the inhibition of nitric oxide production. The optimized CAE hydrogel patch showed strong inhibitory activity with an IC_{50} value of 21.36 ± 0.78 μg/mL. Prednisolone, a positive control exerted excellent inhibitory activity with an IC_{50} value of 1.22 ± 0.07 μg/mL. On the other hand, the cyclooxygenase-inhibiting non-steroidal anti-inflammatory drug (diclofenac) was not active through this pathway. Lycorine, a major component of *C. asiaticum* L., revealed highly potent activity with an IC_{50} value of 0.41 ± 0.01 μg/mL.

Cytotoxicity was determined by MTT assay as shown in Table 7, all samples were not toxic at all concentrations. Therefore, the optimized CAE hydrogel patch had a potent anti-inflammatory effect and is suitable for further development for anti-inflammatory action.

DISCUSSION

Inflammation is a normal response of tissue against infection, cell injury, and damage. Proinflammatory mediators produced during the inflammatory process cause damage to cells, tissues, and organs. Regarding the pathophysiology of osteoarthritis, nitric oxide, tumor necrosis factor-alpha, and prostaglandin E_2 can lead to cartilage and joint degeneration (3,33).

In Thai traditional medicine, *C. asiaticum* L. has long been used to treat inflamed joints and relieve pain (9). Our previous study reported that the ethanolic CAE exerted anti-inflammatory activity (11). Moreover, the CAE also showed significant anti-inflammatory and antinociceptive effects *in vivo* (13,34). Lycorine is one of the major *Crinum* alkaloids

that has potent anti-tumor, immunological, and anti-inflammatory activities (14-16). Thus, these results support *C. asiaticum* L. as a suitable candidate to be further developed as a topical product to treat joint pain and osteoarthritis.

In Thai folk medicine practitioners have long used *C. asiaticum* L. by grilling on a charcoal stove and then wrapping the medicine in the afflicted area that has pain (18). Nevertheless, this form and treatment is inconvenient to use and not a standardized therapeutic in Western medicine. Topical forms such as herbal ball compress, oils, gels, and creams have significant advantages in their use, but they also have disadvantages like uncontrolled drug release and decreased efficacy when adhered to a cloth. Our study was designed to fill this gap in knowledge and formulation. We developed a hydrogel patch that has advantages such as low frequency of application, controlled drug release, prolonged duration of action, and is more convenient to use and portable (20,21). Moreover, a hydrogel patch has a potential therapeutic advantage as the cooling of the hydrogel may also facilitate reduced inflammation.

Importantly, this is the first report of developing a hydrogel patch from carrageenan, locust bean gum, KCl, and glycerin-containing CAE by using the design of the experiment approach. Carrageenan and locust bean gum biopolymers have been widely used in food, cosmetics, and pharmaceuticals (35,36). Furthermore, KCl as an enhancer of gel strength (37) and glycerin as a plasticizer made a flexible film for ease of administration (38). In this study, the combined effect of process variables such as carrageenan, locust bean gum, and glycerin at different levels of the dependent variable (tensile strength) was studied by using the RSM of BBD for design and optimization. In a statistical analysis of the RSM based on BBD, the model was considered reliable and provided functional utility when the regression was significant and a non-significant lack of fit was obtained for the selected confidence level (23). Our study showed that the quadratic model was the best fit for the response tensile strength ($P < 0.0001$) with $R^2 = 0.9742$. This result is beneficial in that it can be used to develop a hydrogel patch containing CAE in the next design optimization and which may be extended to scale for product manufacturing.

Our study showed the effect of variables including carrageenan, locust bean gum, and glycerin on the tensile strength of CAE hydrogel patches as the quadratic equation (1) and 3D response surface plots, carrageenan, and locust bean gum have positive effects on the tensile strength of hydrogel patches. Carrageenan had a greater influence on the hydrogel patch's tensile strength than locust bean gum. However, when glycerin increased the tensile strength, the response decreased. A previous study also supports these results that the tensile strength was decreased, while percent elongation was increased by adding glycerol as a plasticizer (38).

The interaction factors carrageenan: locust bean gum, carrageenan: glycerin, and locust bean gum: glycerin have synergistic effects on increasing tensile strength. However, an excess of each carrageenan, locust bean gum, and glycerin can decrease the tensile strength of hydrogel patches. Hydrogel patch that was produced from only carrageenan or locus bean gum is comparatively weak and easily torn. This is consistent with the findings of Rinanda *et al.* who reported that the biodegradable film from carbohydrates is also easily torn (39). Considering, the 3D response surface plots (Fig. 2A) confirmed that only with the excess of carrageenan, it demonstrated the hard, brittle, and fragile polymer tends to decrease the tensile strength but correspondingly increasing the amount of carrageenan and locust bean gum affected the tendency to increase the tensile strength. Carrageenan is a synergist with locust bean gum and provided a more flexible and stronger hydrogel patch (40,41). Thus, the co-polymer and cross-linker are necessary to be added to strengthen the hydrogel patch.

Glycerin as a plasticizer decreased tensile strength and increased flexible films due to its ability to reduce intermolecular forces between polymer chains (42,43). In this study, glycerin decreased tensile strength at the mid-point of carrageenan and the lowest level of locust bean gum (Fig. 2C). Due to carrageenan and locust bean gum ability as thickening agent films, the low amount of both gums weakened the

hydrogel patch. In the case of locust bean gum, increasing amounts of glycerin at high levels of locust bean gum and mid-point of carrageenan increased tensile strength indicating that the amount of carrageenan is suitable for hydrogel patch forming, when added in a high amount the locust bean gum will be hard and easily broken. So, in this case, glycerin made the hydrogel soft, not easily broken or brittle. Thus, it could be suggested that RSM for the design of experiments should be used to optimize the number of factors to obtain the optimal tensile strength to ensure the physical stability of the hydrogel patch is maintained.

From optimization, the optimized CAE hydrogel patch showed good physical properties, strength, and flexibility. Moreover, the optimized CAE hydrogel patch had the required mechanical properties which showed a good correlation between observed and predicted optimized formulation and tensile strength.

In the *in vitro* release and permeation studies, the optimized CAE hydrogel patch demonstrated the highest lycorine content and cumulative lycorine release. In contrast, F5 (high carrageenan proportion) and F6 (high locust bean gum proportion) showed a lower cumulative lycorine release. Carrageenan and locust bean gum are often used as a thickening and stabilizing agent (44) which has revealed that an increase in the concentration of locust bean gum decreases the cumulative percent drug release with a sustained release (45,46). Kaur *et al*. reported that increasing concentration of locust bean gum and montmorillonite sustained the release of curcumin from k-carrageenan, locust bean gum, and montmorillonite film (45). This study suggested that the optimized CAE hydrogel patch composed of a lower total polymer proportion, led to high erosion and dissolution of the hydrogel patch and thereby facilitated rapid drug release from the hydrogel patch. According to this result, the optimized CAE hydrogel patch showed the highest cumulative lycorine release. The release kinetics model of the optimized CAE hydrogel patch exerted a better fit to Higuchi's model. The optimized CAE hydrogel patch exhibited a burst release in the first 30 min and prolonged release at 6 h, which is advantageous for anti-inflammatory products with rapid initial drug release and prolonged drug release.

The *in vitro* skin permeation of the optimized CAE hydrogel patch showed a high cumulative and prolonged lycorine permeation at 24 h. Moreover, the optimized CAE hydrogel patch contained glycerin as a plasticizer and as a penetration enhancer to increase skin permeability (47,48). Thus, the optimized CAE hydrogel patch not only showed a significant release of drug through the membrane but likewise, it also permeated through pig ear skin as shown in the release and permeation profiles.

This study is the first report on the evaluation of physicochemical properties such as SEM, FTIR, DSC, and XRD of hydrogel patches containing CAE. The optimized CAE hydrogel patch provided a physically stable hydrogel patch and also enabled a completely loaded CAE within the hydrogel patch. From SEM images, a blank-hydrogel patch had a smooth surface indicating that compatible with all ingredients of hydrogel base, while the optimized CAE hydrogel patch showed several vesicles indicating that CAE was completely loaded in the hydrogel patch matrix.

The FTIR spectrum of the blank hydrogel patch showed the characteristic bands positions of carrageenan and locust bean gum as well as the vibration of O-H, C-H stretching and ester sulfate groups (spectrum of carrageenan) and vibration of O-H, aliphatic C-H (spectrum of locust bean gum). Results were similar to previous studies reported for a spectrum of carrageenan and locust bean gum (41,45,49). Our study revealed the chemical interaction between carrageenan and locust bean gum by the shift in peaks corresponding to the C-O stretching band of the C-O-H group band from 1155 cm^{-1} (carrageenan) to 1151 cm^{-1} (blank hydrogel patch) may be due to the interaction through hydrogen bridges between the OH groups of locust bean gum with k-carrageenan structure (41). FTIR spectra of the optimized CAE hydrogel patch showed similar characteristic band positions with CAE extract and lycorine corresponding to the structure and functional groups of lycorine (50-52). This study suggested that carrageenan and locust bean gum synergistically interact in the

formation of the hydrogel patch. The alkaloid lycorine, an active marker of CAE extract, was identified to be able to disperse in the hydrogel patch matrix.

The DSC thermogram analysis showed the blank hydrogel patch had an endothermic peak between those of the pure carrageenan and locust bean gum. The melting point of the blank hydrogel patch was observed higher than carrageenan and locust bean gum powder, it could be explained by synergistic effects between carrageenan and locust bean gum that increased gel strength, and good film-forming properties (53,54). Moreover, potassium ions from KCl have specific site-binding to k-carrageenan that affects the aggregation forming a rigid and brittle hydrogel patch (55-57). The optimized CAE hydrogel patch showed a melting point slightly less than the blank hydrogel patch. However, no disguised signal was found in both DSC thermograms indicating that all the constituents in the blank and optimized CAE hydrogel patch were compatible.

The XRD study revealed that the blank hydrogel patch and optimized CAE hydrogel patch showed a broad diffraction region at 20° (2θ) and no sharp peaks representing their amorphous characters. These results are in agreement with previous studies, carrageenan/locust bean gum blend showed a broad diffraction peak at 20° (2θ) (41). In addition, a previous study reported that the amorphous region leads to enhanced drug diffusion (58). Thus, the amorphous portion of the optimized CAE hydrogel patch exploited the drug release, which could imply good lycorine release.

The optimized CAE hydrogel patch showed a suitable physical appearance, mechanical properties and also showed strong anti-inflammatory activity by inhibition of nitric oxide production from RAW 264.7 cells with an IC_{50} value of 21.36 ± 0.78 µg/mL. Even in the form of a product containing a hydrogel base the anti-inflammatory effect is similar to the anti-inflammatory effect of the CAE extract (IC_{50} = 16.66 ± 1.42 µg/mL) (11). Moreover, it showed activity through the effect of CAE was not the base of the hydrogel patch (blank hydrogel patch) as the blank hydrogel patch was not active on inhibitory nitric oxide production. Although its anti-inflammatory effect was significantly less than prednisolone, clinical use of prednisolone has long-term corticosteroid side effects (7). Additionally, the optimized CAE hydrogel patch was not toxic at any of the used concentrations as determined by the MTT assay.

Therefore, the optimized CAE hydrogel patch had potent anti-inflammatory activity by inhibiting nitric oxide production from RAW 264.7 cells. Nitric oxide is a mediator with important roles in the pathogenesis of inflammatory disease and has a destructive effect on articular cartilage leading to osteoarthritis. Thus, the optimized CAE hydrogel patch may be suitable to use as herbal medicine hydrogel patch for anti-inflammatory relief in osteoarthritis. However, further animal models to evaluate the edema, pain reduction, and skin irritation of this hydrogel patch towards clinical development should be undertaken. Interestingly, this study provided a guided design approach to successfully develop hydrogel patches based on carrageenan, locust bean gum, KCl, glycerin, and containing CAE as a topical anti-inflammatory drug.

CONCLUSION

This study prepared *C. asiaticum* L. hydrogel patches designed by using RSM (BBD) including three factors carrageenan, locust bean gum, and glycerin. The tensile strength was selected as the key parameter to be optimized. The optimized CAE hydrogel patch demonstrated excellent physical appearance, mechanical properties, high lycorine content, cumulative release, and skin permeation. The evaluated physicochemical properties including SEM, DSC, and XRD revealed the homogeneity, compatibility, and crystallinity of all ingredients. From FTIR, lycorine which was the marker of CAE extract was identified and dispersed in the hydrogel patch matrix. Moreover, the optimized CAE hydrogel patch showed an anti-inflammatory effect *in vitro*. Thus, this study supports the traditional use of *C. asiaticum* L. to relieve joint inflammation and pain and the optimized CAE hydrogel patch should be further studied in the animal models and clinical trials for topical applications for inflammation and relief of pain in osteoarthritis.

Acknowledgements

This research was supported by Thailand Science Research and Innovation (TSRI) through the Royal Golden Jubilee Ph.D. Program (Grant No. PHD/0078/2558) and National Research Council of Thailand, the Thailand Science Research and Innovation Fundamental Fund and Center of Excellence in Applied Thai Traditional Medicine Research (CEATMR), Faculty of Medicine, Thammasat University, for financial support and the use of laboratory facilities. Dr. Davies is a Bualang ASEAN Chair Professor. The authors are grateful to the Department of Biotechnology, the Korea National University of Transportation for providing the facilities to develop and study the hydrogel patch. Thank DKSH Thailand for support using XRD analytical.

Conflicts of interest statement

The authors declared that they have no conflicts of interest in this study.

Authors' contributions

A. Itharat conceived and supervised the project. C. Kongkwamcharoen performed the experiments, analyzed the data, and wrote the manuscript in consultation with A. Itharat, W. Ketjinda, and N.M. Davies. H.Y. Lee provided the facilities and technical methods for developing and evaluating hydrogel patches. G.S. Moon provided the facilities and experimental design. W. Ketjinda advised the experimental design and verified the analytical methods. N.M. Davies provided scientific, statistical, modeling, technical, and grammatical amendments to the manuscript. All authors read and approved the final version of the manuscript.

REFERENCES

1. Di Nicola V. Degenerative osteoarthritis a reversible chronic disease. Regen Ther. 2020; 15:149-160.
   DOI: 10.1016/j.reth.2020.07.007.
2. Wright HL, Moots RJ, Bucknall RC, Edwards SW. Neutrophil function in inflammation and inflammatory diseases. Rheumatology (Oxford). 2010;49(9):1618-1631.
   DOI: 10.1093/rheumatology/keq045.
3. Chow YY, Chin KY. The role of inflammation in the pathogenesis of osteoarthritis. Mediators Inflamm. 2020; 2020:8293921,1-19.
   DOI: 10.1155/2020/8293921.
4. Berenbaum F, Walker C. Osteoarthritis and inflammation: a serious disease with overlapping phenotypic patterns. Postgrad Med. 2020;132(4):377-384.
   DOI: 10.1080/00325481.2020.1730669.
5. Wongrakpanich S, Wongrakpanich P, Melhado K, Rangaswami J. A comprehensive review of non-steroidal anti-inflammatory drug use in the elderly. Aging Dis. 2018;9(1):143-150.
   DOI: 10.14336/AD.2017.0306.
6. Makris UE, Kohler MJ, Fraenkel L. Adverse effects of topical nonsteroidal anti-inflammatory drugs in older adults with osteoarthritis: a systematic literature review. J Rheumatol. 2010;37(6):1236-1243.
   DOI: 10.3899/jrheum.090935.
7. Poetker DM, Reh DD. A comprehensive review of the adverse effects of systemic corticosteroids. Otolaryngol Clin North Am. 2010;43(4):753-768.
   DOI: 10.1016/j.otc.2010.04.003.
8. Haque M, Jahan S, Rahmatullah M. Ethnomedicinal uses of *Crinum asiaticum*: a review. World J Pharm Pharm Sci. 2014;3(9):119-128.
9. Pichiansunthorn C, Chawalit M, Jeerawong V. The describe of Osod Phra Narai textbook. Bangkok: Amarin Publishing; 2001. pp. 221–227.
10. Ghane SG, Attara UA, Yadav PB, Lekhak MM. Antioxidant, anti-diabetic, acetylcholinesterase inhibitory potential and estimation of alkaloids (lycorine and galanthamine) from *Crinum* species: An important source of anticancer and anti-Alzheimer drug. Ind Crops Prod. 2018;125:168-177.
    DOI: 10.1016/j.indcrop.2018.08.087.
11. Kongkwamcharoen C, Itharat A, Pipatrattanaseree W, Ooraikul B. Effects of various preextraction treatments of *Crinum asiaticum* leaf on its anti-inflammatory activity and chemical properties. Evid Based Complement Alternat Med. 2021; 2021:8850744,1-11.
    DOI: 10.1155/2021/8850744.
12. Mahomoodally MF, Sadeer NB, Suroowan S, Jugreet S, Lobine D, Rengasamy KRR. Ethnomedicinal, phytochemistry, toxicity and pharmacological benefits of poison bulb *Crinum asiaticum* L. S Afr J Bot. 2021;136:16-29.
    DOI: 10.1016/j.sajb.2020.06.004.
13. Rahman MA, Hossain SMA, Ahmed N, Islam MS. Analgesic and anti-inflammatory effects of *Crinum asiaticum* leaf alcoholic extract in animal models. Afr J Biotechnol. 2013;12(2):212-218.
    DOI: 10.5897/AJB12.1431.
14. Ji YB, Tian P, Dai QC, Wang ST, Chen N. The present research situation of *Crinum asiaticum* alkaloids active ingredient. Appl Mech Mater. 2013;411-414:3181-3186.
    DOI: 10.4028/www.scientific.net/amm.411-414.3181.
15. Khalifa MF, Shihata EZA, Refaat J, Kamel MS. An overview on the chemical and biological aspects of lycorine alkaloid. J Adv Biomed Pharm Sci. 2018;1(2):41-49.
    DOI: 10.21608/JABPS.2018.4088.1016.
16. Kang J, Zhang Y, Cao X, Fan J, Li G, Wang Q, *et al*. Lycorine inhibits lipopolysaccharide-induced iNOS

and COX-2 up-regulation in RAW264.7 cells through suppressing P38 and STATs activation and increases the survival rate of mice after LPS challenge. Int Immunopharmacol. 2012;12(1): 249-256.
DOI: 10.1016/j.intimp.2011.11.018.
17. Park HJ, Zadeh MG, Suh JH, Choi HS. Lycorine attenuates autophagy in osteoclasts *via* an axis of mROS/TRPML1/TFEB to reduce LPS-induced bone loss. Oxid Med Cell Longev. 2019; 2019:8982147, 1-11.
DOI: 10.1155/2019/8982147.
18. Department of Thai Traditional and Alternative Medicine, Guidelines for Certification of Folk Medicine. Bangkok: Thailand Ministry Publishing; 2019. pp. 1-80.
19. Stanos SP, Galluzzi KE. Topical therapies in the management of chronic pain. Postgrad Med. 2013; 125:25-33.
DOI: 10.1080/00325481.2013.1110567111.
20. Nalamachu S, Gudin J. Characteristics of analgesic patch formulations. J Pain Res. 2020; 13:2343-2354.
DOI: 10.2147/JPR.S270169.
21. Nilforoushzadeh MA, Amirkhani MA, Zarrintaj P, Salehi Moghadam A, Mehrabi T, Alavi S, *et al*. Skin care and rejuvenation by cosmeceutical facial mask. J Cosmet Dermatol. 2018;17(5):693-702.
DOI: 10.1111/jocd.12730.
22. Bezerra MA, Santelli RE, Oliveira EP, Villar LS, Escaleira LA. Response surface methodology (RSM) as a tool for optimization in analytical chemistry. Talanta. 2008;76(5):965-977.
DOI: 10.1016/j.talanta.2008.05.019.
23. Candioti LV, De Zan MM, Camara MS, Goichoechea HC. Experimental design and multiple response optimization. Using the desirability function in analytical methods development. Talanta. 2014; 124:123-138.
DOI: 10.1016/j.talanta.2014.01.034.
24. Fukuda IM, Pinto CFF, Moreira CDS, Saviano AM, Lourenco FR. Design of experiments (DoE) applied to pharmaceutical and analytical quality by design (QbD). Braz J Pharm Sci. 2018;54:e01006,1-16.
DOI: 10.1590/s2175-97902018000001006.
25. Dhoot AS, Fernandes GJ, Naha A, Rathnanand M, Kumar L. Design of experiments in pharmaceutical development. Pharm Chem J. 2019;53(8):730-735.
DOI: 10.1007/s11094-019-02070-4.
26. Choudhary V, Shivakumar H, Ojha H. Curcumin-loaded liposomes for wound healing: preparation, optimization, *in-vivo* skin permeation and bio evaluation. J Drug Deliv Sci Technol. 2018; 49:683-691.
DOI: 10.1016/j.jddst.2018.12.008.
27. Parhi, R, Suresh P, Patnaik S. Application of response surface methodology for design and optimization of reservoir-type transdermal patch of simvastatin. Curr Drug Deliv. 2016;13(5):742-753.
DOI: 10.2174/1567201812666151009115944.
28. Achirasena W, Ketjinda W, Sakunphueak A. Formulation and physical evaluation of topical patch containing Derris scandens. Interprof J Health Sci. 2018;16(2):135-146.
DOI: 10.14456/ijhs.2018.5.
29. Suksaeree J, Nawathong N, Anakkawee R, Pichayakorn W. Formulation of polyherbal patches based on polyvinyl alcohol and hydroxypropylmethyl cellulose: characterization and *in vitro* evaluation. AAPS Pharm Sci Tech. 2017;18(7):2427-2436.
DOI: 10.1208/s12249-017-0726-0.
30. Patel NA, Patel NJ, Patel RP. Design and evaluation of transdermal drug delivery system for curcumin as an anti-inflammatory drug. Drug Dev Ind Pharm. 2009;35(2):234-242.
DOI: 10.1080/03639040802266782.
31. Raknam P, Pinsuwan S, Amnuaikit T. Phenylethyl resorcinol loaded in liposomal cream formulation for cosmeceutical application. J Pharm Res Int. 2020;32(1):64-76.
DOI: 10.9734/JPRI/2020/v32i130396.
32. Makchuchit S, Rattarom R, Itharat A. The anti-allergic and anti-inflammatory effects of Benjakul extract (a Thai traditional medicine), its constituent plants and its some pure constituents using *in vitro* experiments. Biomed Pharmacother. 2017; 89:1018-1026.
DOI: 10.1016/j.biopha.2017.02.066.
33. Kapoor M, Martel-Pelletier J, Lajeunesse D, Pelletier JP, Fahmi H. Role of proinflammatory cytokines in the pathophysiology of osteoarthritis. Nat Rev Rheumatol. 2011;7(1):33-42.
DOI: 10.1038/nrrheum.2010.196.
34. Asmawi MZ, Arafat OM, Amirin S, Eldeen IMS. *in vivo* antinociceptive activity of leaf extract of *Crinum asiaticum* and phytochemical analysis of the bioactive fractions. Int J Pharmacol. 2011;7(1):125-129.
DOI: 10.3923/ijp.2011.125.129.
35. Petitjean M, Isasi JR. Locust bean gum, a vegetable hydrocolloid with industrial and biopharmaceutical applications. Molecules. 2022;27(23):8265,1-17.
DOI: 10.3390/molecules27238265.
36. de Jesus Raposo MF, de Morais AMB, de Morais RMSC. Marine polysaccharides from algae with potential biomedical applications. Mar Drugs. 2015;13(5):2967-3028.
DOI:10.3390/md13052967.
37. Zhu Y, Bhandari B, Prakash S. Tribo-rheometry behaviour and gel strength of κ-carrageenan and gelatin solutions at concentrations, pH and ionic conditions used in dairy products. Food Hydrocoll. 2018;84:292-302.
DOI: 10.1016/j.foodhyd.2018.06.016.
38. Jantrawut P, Chaiwarit T, Jantanasakulwong T, Brachais CH, Chambin O. Effect of plasticizer type on tensile property and *in vitro* indomethacin release of thin films based on low-methoxyl pectin. Polymers. 2017;9(7):289-293.
DOI: 10.3390/polym9070289.
39. Rinanda SA, Nastabiq M, Raharjo SH, Hayati SK, Yaqin MA, Ratnawati. The effect of combination of sugar palm fruit, carrageenan, and citric acid on mechanical properties of biodegradable film. J Phys Conf Ser. 2017;909(1):012085,1-5.
DOI:10.1088/1742-6596/909/1/012085.

40. Barak S, Mudgil D. Locust bean gum: processing, properties and food applications- a review. Int J Biol Macromol. 2014;66:74-80.
DOI: 10.1016/j.ijbiomac.2014.02.017.
41. Martins JT, Cerqueira MA, Bourbon AI, Pinheiro AC, Souza BWS, Vicente AA. Synergistic effects between k-carrageenan and locust bean gum on physicochemical properties of edible films made thereof. Food Hydrocoll. 2012;29(2):280-289.
DOI: 10.1016/J.FOODHYD.2012.03.004.
42. Ballesteros-Mártinez L, Pérez-Cervera C, Andrade-Pizarro R. Effect of glycerol and sorbitol concentrations on mechanical, optical, and barrier properties of sweet potato starch film. NFS J. 2020;20:1-9.
DOI: 10.1016/j.nfs.2020.06.002.
43. Tarique J, Sapuan SM, Khalina A. Effect of glycerol plasticizer loading on the physical, mechanical, thermal, and barrier properties of arrowroot (*Maranta arundinacea*) starch biopolymers. Sci Rep. 2021;11(1):13900,1-17.
DOI: 10.1038/s41598-021-93094-y.
44. Dionisio M, Grenha A. Locust bean gum: Exploring its potential for biopharmaceutical applications. J Pharm Bioallied Sci. 2012;4(3):175-185.
DOI: 10.4103/0975-7406.99013.
45. Kaur R, Sharma A, Puri V, Singh I. Preparation and characterization of biocomposite films of carrageenan/locust bean gum/montmorrillonite for transdermal delivery of curcumin. Bioimpacts. 2019; 9(1):37-43.
DOI: 10.15171/bi.2019.05.
46. Biswas D, Das S, Mohanto S., Mantry S. Extraction, modification, and characterization of natural polymers used in transdermal drug delivery system: an updated review. Asian J Pharm Clin Res. 2020;13(7):10-20.
DOI: 10.22159/ajpcr.2020.v13i7.37756.
47. Bjorklund S, Engblom J, Thuresson K., Sparr E. Glycerol and urea can be used to increase skin permeability in reduced hydration conditions. Eur J Pharm Sci. 2013;50(5):638-645.
DOI: 10.1016/j.ejps.2013.04.022.
48. Pichayakorn W, Suksaere J, Boonme P, Amnuaikit T, Taweepreda W, Ritthidej GC. Nicotine transdermal patches using polymeric natural rubber as the matrix controlling system: effect of polymer and plasticizer blends. J Membr Sci. 2012;411-412:81-90.
DOI: 10.1016/j.memsci.2012.04.017.
49. Pettinelli N, Rodriguez-Llamazares S, Bouza R, Barral L, Feijoo-Bandin S, Lago F. Carrageenan-based physically crosslinked injectable hydrogel for wound healing and tissue repairing applications. Int J Pharm. 2020;589:119828,1-9.
DOI: 10.1016/j.ijpharm.2020.119828.
50. Lamoral-Theys D, Andolfi A, Van Goietsenoven G, Cimmino A, Le Calve B, Wauthoz N, *et al*. Lycorine, the main phenanthridine amaryllidaceae alkaloid, exhibits significant antitumor activity in cancer cells that display resistance to proapoptotic stimuli: an investigation of structure-activity relationship and mechanistic insight. J Med Chem. 2009;52(20):6244-6256.
DOI: 10.1021/jm901031h.
51. Lamoral-Theys D, Decaestecker C, Mathieu V, Dubois J, Kornienko A, Kiss R, *et al*. Lycorine and its derivatives for anticancer drug design. Mini Rev Med Chem. 2010;10(1):41-50.
DOI: 10.2174/138955710791112604.
52. McNulty J, Nair JJ, Bastida J, Pandey S, Griffin C. Structure-activity studies on the lycorine pharmacophore: a potent inducer of apoptosis in human leukemia cells. Phytochemistry. 2009;70(7):913-919.
DOI: 10.1016/j.phytochem.2009.04.012.
53. Necas J, Bartosikova L. Carrageenan: a review. Vet Med. 2013;58(4):187-205.
DOI: 10.17221/6758-VETMED.
54. Yuan L, Wu Y, Qin Y, Yong H, Liu J. Recent advances in the preparation, characterization and applications of locust bean gum-based films. J Renew Mater. 2020;8(12):1565-1579.
DOI: 10.32604/jrm.2020.014562.
55. Williams PA. Molecular interactions of plant and algal polysaccharides. Struct Chem. 2009;20(2):299-308.
DOI: 10.1007/s11224-009-9420-5.
56. Nguyen BT, Nicolai T, Benyahia L, Chassenieux C. Synergistic effects of mixed salt on the gelation of κ-carrageenan. Carbohydr Polym. 2014;112:10-15.
DOI: 10.1016/j.carbpol.2014.05.048.
57. Pacheco-Quito EM, Ruiz-Caro R, Veiga MD. Carrageenan: drug delivery systems and other biomedical applications. Mar Drugs. 2020;18(11):583,1-39.
DOI: 10.3390/md18110583.
58. Kamaly N, Yameen B, Wu J, Farokhzad OC. Degradable controlled-release polymers and polymeric nanoparticles: mechanisms of controlling drug release. Chem Rev. 2016;116(4):2602-2663.
DOI: 10.1021/acs.chemrev.5b00346.